Fuel Processing Technology 104 (2012) 325–331

Contents lists available at SciVerse ScienceDirect

Fuel Processing Technology

journal homepage: www.elsevier.com/locate/fuproc

The effects of Cu/HZSM-5 on combined removal of Hg^0 and NO from flue gas

Xiaopeng Fan, Caiting Li *, Guangming Zeng, Xing Zhang, Shasha Tao, Pei Lu, Shanhong Li, Yapei Zhao

College of Environmental Science and Engineering, Hunan University, Changsha 410082, PR China
Key Laboratory of Environmental Biology and Pollution Control (Hunan University), Ministry of Education, Changsha 410082, PR China

ARTICLE INFO

Article history:
Received 30 October 2011
Received in revised form 23 May 2012
Accepted 2 June 2012
Available online 21 June 2012

Keywords:
Elemental mercury
Nitrogen oxide
HZSM-5
Copper

ABSTRACT

The combined removals of Hg^0 and NO over zeolite (HZSM-5 was chosen to use) modified by copper (Cu/HZSM-5) catalysts were studied under different simulated flue gas conditions. Compared with HZSM-5, Cu/HZSM-5 showed higher activity and performed a synergetic effect for the Hg^0 and NO removal at 250 °C. But the excess of copper could cause destruction of the thin pore walls and blocking of internal porosity of the catalyst leading to decrease of the activity. A comparison between Cu/HZSM-5 of different silica to alumina ratios (SiO_2/Al_2O_3 ratio) was also performed. The highest NO and Hg^0 conversions were observed over the lowest SiO_2/Al_2O_3 ratio. In addition, the experimental results indicated that there was a synergetic effect between HZSM-5 and copper for the removal of NO and Hg^0 by accelerating the intermediate formation (NO_2) and by strengthening the adsorption NO and Hg^0 on the catalyst surface under the reaction conditions. Moreover, the effects of individual flue gas components on the removals of Hg^0 and NO were examined. O_2 in the flue gas had a positive effect on both Hg^0 and NO removals. However, the presence of H_2O and SO_2 inhibited both Hg^0 and NO removals.

1. Introduction

It has been reported that mercury emissions cause more and more adverse effects on environment and human health because of its high toxicity, volatility, and bioaccumulation [1–3]. According to reports, the mercury emissions from coal-fired plant account for approximately one-third of the anthropogenic mercury emissions [4]. Consequently, development of technologies governing/controlling the mercury emission from coal-fired power plants has become an urgent issue for the countries using coal as their principal energy.

Mercury in coal-fired flue gas is often presented as three chemical forms: element mercury (Hg^0), oxidized mercury (Hg^{2+}), and particle-bound mercury (Hg^p) [5]. With consideration of the properties of Hg^{2+}, Hg^p, and Hg^0, studies of the Hg^0 removal method should be firstly taken into account. Many current researches on controlling Hg^0 emission from flue gas mainly focus on injecting sorbent and promoting Hg^0 oxidation. Among those schemes, sorbent injection is the current reference technology for the control of mercury in a coal-fired utility plant [6,7]. However, obvious disadvantages such as higher operation expenses, poor capacity, narrow temperature range of application and slow regeneration and adsorption rates are proven using this technology, which limit its wide application [8]. Therefore, promoting the Hg^0 oxidation exhibits a promising future on the basis that Hg^{2+} can be removed through currently available pollution control devices. Recently, some transition-metal oxides, such as Fe_2O_3, V_2O_5, CuO, CeO_2, Mn_2O_3, and RuO_2 have been extensively investigated as potential Hg^0 oxidation catalysts, and it has been observed that these metal oxides were helpful to the oxidation of Hg^0 to Hg^{2+} [9–12]. In addition, it has been proven that commercial catalysts used in selective catalytic reduction (SCR) of NO with NH_3 which has been investigated for several years and is today a well established technique for DeNOx in stationary applications, have some promotion for the oxidation of Hg^0 [13]. However, the predictability of the removal extent is unreliable [14,15]. Thus, it encourages us to search for a suitable catalyst which not only has higher NO removal efficiency, but also can promote the Hg^0 removal from the flue gas. A number of SCR catalysts have been proposed in literature; however, among them, Cu/HZSM-5 catalysts have been extensively studied and attracted a great deal of attention as potential catalysts for NH_3-SCR. Compared to other previously studied materials, the Cu/HZSM-5 exhibits a significant enhancement both in terms of the conversion rate and selectivity [16–18]. In previous works, it was reported that HZSM-5 which had higher mechanical strength, chemical and thermal stability performed high active on Hg^0 removal from flue gas [19]. Moreover, copper was found to have superior activity and stability on Hg^0 capture [20,21]. Those results made us to speculate that the Hg^0 could be efficiently controlled over Cu/HZSM-5 in SCR systems. Therefore, in this work, Cu/HZSM-5 was developed and some related experiments including SiO_2/Al_2O_3 ratio, reaction temperature, CuO loading value and flue gas component on NO and Hg^0 removal efficiencies were evaluated in a lab-scale SCR system.

* Corresponding author. Tel./ fax: +86 731 888649216.
E-mail address: ctli3@yahoo.com (C. Li).

0378-3820/$ – see front matter.
doi:10.1016/j.fuproc.2012.06.003

2. Materials and methods

2.1. Sample preparation

Commercially available HZSM-5 (with SiO_2/Al_2O_3 ratio of 25, 50, and 100) purchased from NanKai University was used in this study as parent zeolites. The Cu/HZSM-5 was prepared by incipient wetness impregnation method as follows: First, the $Cu(NO_3)_3 \cdot 6H_2O$ was dissolved in de-ionized water to form the solution. Then, HZSM-5 was added to the solution with stirring in a proportion corresponding to different loading values (ρ, where ρ is the mass ratio of Cu to HZSM-5) varying from 3 to 12##wt%. Third, the samples were dried in an electric blast drying oven at 120 °C for 24##h and then calcined at 450 °C in air for 5 h. The obtained samples, designated as ρ Cu/HZSM-5 (*A*) (where "*A*" denotes the SiO_2/Al_2O_3 ratio) were crushed and sieved to 40–60 mesh particles for future use.

2.2. Analytical methods

The Brunauer–Emmet–Teller (BET) of the samples was determined by nitrogen adsorption at −196 °C on a Micromeritics ASAP 2010 analyzer. The pore size distribution was characterized using the desorption branches of the N_2 adsorption isotherm and the Barrett–Joyner–Halenda (BJH) formula. All the samples were degassed at 120 °C prior to BET measurements. The scanning electron microscope (SEM) photographs of the samples were obtained by means of JSM-6700 F after vacuum plating Au film. The powder X-ray diffraction (XRD) measurements were carried out with a Rigaku Rotaflex D/Max-C system with Cu Kα ($\lambda = 0.1543$ nm) radiation. The samples were loaded on a sample holder with a depth of 1 mm. Thermogravimetric analysis (TG; STA-409PC/PG) was used to determine the speciation of mercury deposits on used samples. In order to expedite the experiment so that the capacity of the composite material could be more easily tested, the samples were firstly exposed to the simulated flue gas with 200 μg/m^3 Hg^0 about 400 h. For each test, about 10-mg samples were heated from the room temperature to 800 °C at the heating rates of 10 °C/min under nitrogen atmosphere (>99.99%). And the flow rate of N_2 was kept both at 100 ml/min to ensure an inert atmosphere during the run. NO and NO_x concentrations in the inlet and outlet gases were measured by KM900 Hand–held Combustion Analyser (Kane International Limited, UK.). Hg^0 concentrations in vapor phase were analyzed by the RA-915 Portable Mercury Analyzer (with a detection limit of 0.002 μg/m^3, it has a nominal range of 0.002–20 μg/m^3), which is based on differential Zeeman atomic absorption spectrometry using high-frequency modulation of light polarization.

2.3. Catalytic test

A schematic diagram of the experimental setup is shown in Fig. 1. The apparatus consisted of a simulated flue gas system, a fixed-bed reactor, and a gas analyzer system including an Hg^0 analyzer and a NO analyzer. The composition of the basic flue gas included 5% O_2, 1000 ppm NO, 1200 ppm NH_3, 900 ppm SO_2, 12% CO_2, and the balance N_2. The N_2 flow was divided into two branches: one branch converged with the NO, CO_2, SO_2, NH_3, and O_2 to form the main gas flow, while the other passed (150 ml/min) through an Hg^0 permeation tube (VICI Metronics) and introduced the saturated Hg^0 vapor into the system. The Hg^0 permeation tube was placed in a U-shape glass tube, which was immersed in a constant temperature water bath to ensure a constant Hg^0 permeation rate. Hg^0 concentration in the system was controlled at 20.02 μg/m^3. The total flux was controlled at 0.5 l/min in each project using mass flow controller, corresponding to a space velocity of about 10000 h^{-1}.

As quartz had been demonstrated to have good chemical resistance and inertness toward Hg^0, a quartz tube with an inner diameter of 10 mm held in a vertical position was used as the reactor which was surrounded by a large tubular furnace and about 0.1 g of the catalyst was packed in it. A temperature control device was employed to keep the fixed-bed reactor at desired temperature. The inlet and outlet Hg^0 and NO concentrations of the fixed-bed reactor were measured by Hg^0 analyzer and NO analyzer. After the analysis, the exhaust gas emission from the mercury analyzer was introduced into the activated carbon trap before being expelled into the air.

Table 1 summarizes the experimental conditions. Set 1 experiments aimed at determining the optimal operating temperature. The experiments were carried out over a temperature range (150–400 °C) under simulated flue gas. In the second set, the effects of CuO loading value on Hg^0 and NO removal efficiencies were studied using 0, 3, 6, 9 and 12% Cu/HZSM-5 at 250 °C. The roles of SiO_2/Al_2O_3 ratio on Hg^0 and NO removal efficiencies were explored in Set 3 experiments. In sets 4, 5, and 6, the effects of individual flue gas components on Hg^0 and NO removals were studied over 6% Cu/HZSM-5 at 250 °C.

During the experiment, the experimental gas firstly bypassed the quartz tube and was introduced into the catalytic system until the desired inlet mercury concentration had been established for about 20 min. For the whole tests, the Hg^0 removal efficiency (η_{Hg^0}) was

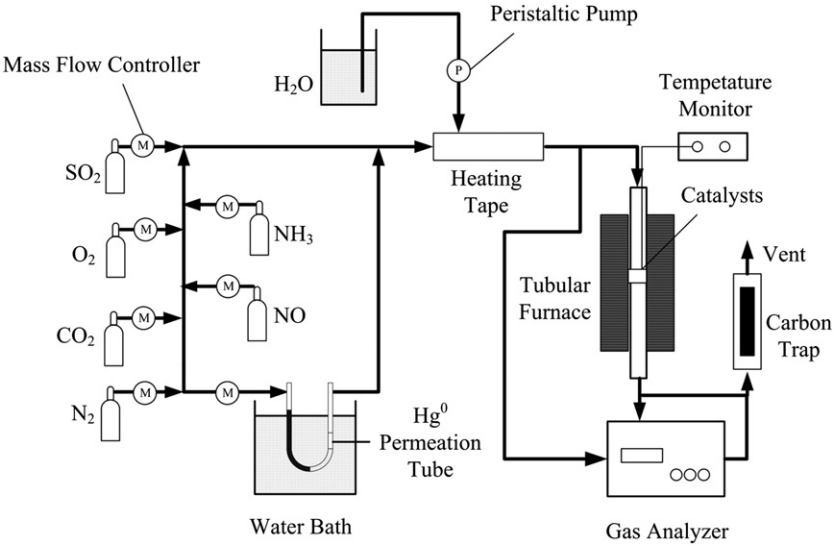

Fig. 1. Schematic diagram of the experimental setup.

Table 1
Experimental conditions.

	Catalyst	SiO2/Al2O3 ratio	Carrier gas (0.5 l/min)		
			O2 (%)	SO2 (ppm)	H2O (%)
Set 1	6% Cu/HZSM-5	25	5	1000	0
Set 2	0% to 12% Cu/HZSM-5	25	5	1000	0
Set 3	6% Cu/HZSM-5	25, 50, 100	5	1000	0
Set 4	6% Cu/HZSM-5	25	5	1000	0, 8
Set 5	6% Cu/HZSM-5	25	0, 5, 8	1000	0
Set 6	6% Cu/HZSM-5	25	5	0, 500, 900	0

All the conditions contained 1000 ppm NO, 1200 ppm NH3, 12% CO2, and balanced N2.

quantified by a comparison between the Hg^0 concentration of the inlet and outlet of the quartz tube. Meanwhile, the NO removal efficiency (η_{NO}) was quantified by a comparison between the NO_x concentration of the inlet and outlet of the quartz tube. η_{Hg^0} and η_{NO} are defined as “”reactions (1) and (2):

$$\eta_{Hg^0} = \frac{Hg^0_{inlet} - Hg^0_{outlet}}{Hg^0_{inlet}} \times 100\% \quad (1)$$

$$\eta_{NO} = \frac{NOx_{inlet} - NOx_{outlet}}{NOx_{inlet}} \times 100\% \quad (2)$$

3. Results and discussion

3.1. Sample characteristics

The BET surface areas (S_{BET}) and volumes of parent and modified HZSM-5 were listed in Table 2. It could be observed that the fresh HZSM-5 had the largest S_{BET} and pore volume, 340 m^2/g and 0.170 cm^3/g, respectively. When the loading value was under 6%, the change of S_{BET} and volume values was lesser. For example, when the Cu loading value changed from 0 to 6%, S_{BET} and the volume decreased only 12 m^2/g and 0.01 cm^3/g, respectively. From these results, one can conclude that textural properties of HZSM-5 were preserved during the catalysts preparation. However, the surface area and volume values of the samples decreased with the continuously increasing of CuO loading value. This could be due to that the existence of agglomerated copper oxide over the external surface of the samples caused destruction of the thin pore walls and blocking of internal porosity.

The results of SEM photographs of pure HZSM-5 and 6% Cu/HZSM-5 (25) were displayed in Fig. 2. The typical coffin-shape of HZSM-5 and the non-crystallographic intracrystalline mesopores resulting in the high porosity and the relatively larger average pore size of the mesoporous zeolite single crystals could be seen for all samples. Otherwise, it could be seen that the surface of HZSM-5 was smooth and the microcrystal was clear, without any adsorbed particle. Comparing Fig. 2(b) with Fig. 2(a), there were more white circled spot on the surface of Cu/HZSM-5, which could ascribe to CuO particles. Meanwhile, these particles were widely dispersed on the HZSM-5 surface and only a few number of agglomerations existed, but its particle size was too small to be recognized. Better dispersion of CuO could account for the higher catalytic activity of mesoporous samples.

Table 2
Specific surface area and volume of the samples.

Samples	BET surface area (m^2/g)	Total pore volume (cm^3/g)
HZSM-5 (25)	340.32	0.170
3% Cu/HZSM-5 (25)	337.27	0.167
6% Cu/HZSM-5 (25)	328.49	0.160
9% Cu/HZSM-5 (25)	272.66	0.150
12% Cu/HZSM-5 (25)	246.80	0.142

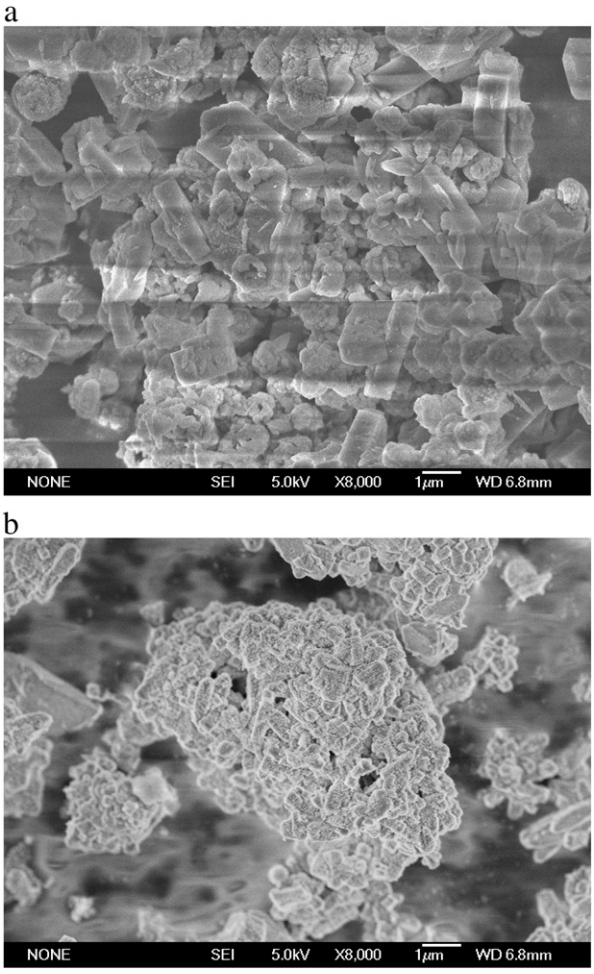

Fig. 2. SEM photographs of (a) HZSM-5 zeolite and (b) 6% Cu/HZSM-5 (25).

The XRD experimental results of HZSM-5 and Cu/HZSM-5 (25) were shown in Fig. 3. The peaks at the ranges of $2\theta = 7–9°$ and 23–25° in the XRD pattern were corresponding to the specific peaks of HZSM-5, which could be detected over all the samples. However, the diffraction peak of CuO crystallites could be detected only when the CuO content was over 6%. It meant that no apparent characteristic peaks ascribable to CuO with lower CuO loading, which indicated that

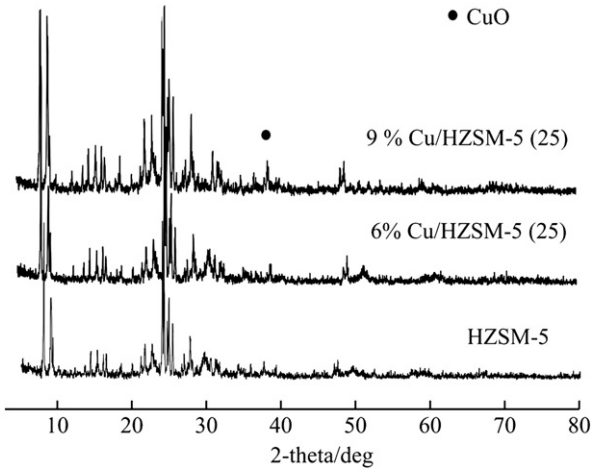

Fig. 3. XRD analyses of the samples.

CuO was highly dispersed on HZSM-5. This result was in accordance with the result of Fig. 2(b) and Table 2.

3.2. Temperature effect

Further investigations on Hg^0 and NO removal efficiencies of 6% Cu/HZSM-5 (25) were carried out as a function of temperature between 150 and 400 °C and the experimental results were shown in Fig. 4. It could be seen that the reaction temperature play a key role on both NO and Hg^0 removal of 6% Cu/HZSM-5 (25). With increasing reaction temperature, the NO removal efficiency increased continuously and reached maximum. However, the Hg^0 removal efficiency was some different. When the reaction temperature increased from 150 °C to 250 °C, the Hg^0 removal efficiency of 6% Cu/HZSM-5 (25) augmented from 60% to 90.2%. But the sustained growth of reaction temperature would lead to a decrease in it. These results indicated that although the elevated temperature benefited the removal of Hg^0, it is unfavorable for the removal of Hg^0 when the temperature exceeded 250 °C. At the temperature of 250 °C, the Hg^0 removal efficiency of 6% Cu/HZSM-5 (25) performed the highest value, and the NO removal efficiency also reached about 90%. These results indicated that 6% Cu/HZSM-5 could achieve very good results on the removal both of Hg^0 and NO at this reaction temperature.

3.3. Effect of loading value

The effects of CuO loading value on the removals of Hg^0 and NO were studied over Cu/HZSM-5 (25) samples at 250 °C. As shown in Fig. 5, copper significantly enhanced the Hg^0 removal ability of HZSM-5. When the CuO loading was lower than 6%, the Hg^0 removal efficiency gradually increased with increasing CuO content. For example, over the HZSM-5, the removal efficiency of Hg^0 was 40%. However, over the 6% Cu/HZSM-5 (25), 90% of Hg^0 conversion was achieved. However, further increase of copper loading led to the activity of the catalyst slightly decrease. The 9% Cu/HZSM-5 (25) catalyst gave 80% of Hg^0 removal efficiency that was obviously lower than the 6% Cu/HZSM-5 (25). The possible reason was that S_{BET} of Cu/HZSM-5 had a great decrease (as shown in Table 2) during the loading value increasing from 6% to 9%, which might affect the Hg^0 removal efficiency of Cu/HZSM-5.

On the other hand, the NO removal efficiency showed the same trend as that of Hg^0. At this temperature, the NO conversion ratio increased and then decreased with the increase of CuO loading value. Over the 6% Cu/HZSM-5 (25), the maximum activity toward the aimed reaction was achieved. Based on the above analysis, it could be found that the maximum activity of Cu/HZSM-5 (25) for the removals of Hg^0 and NO was observed at approximately 6%. Consequently, the reasonable loading value of CuO was chosen as 6% in our later investigation.

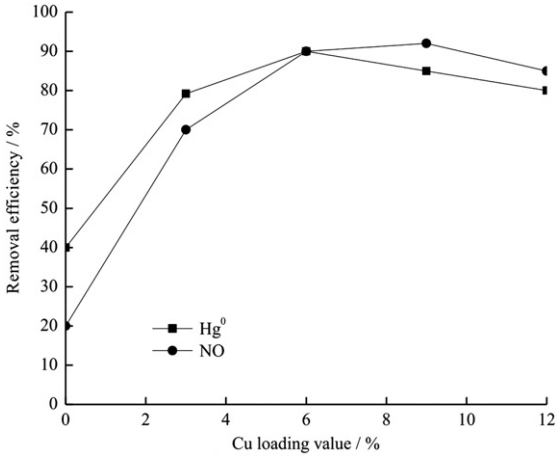

Fig. 5. Effect of the CuO loading value on Hg^0 and NO removal efficiencies of HZSM-5 (25) at 250 °C.

3.4. Effect of the SiO_2/Al_2O_3 ratio

Another important dependence factor for the activity of Cu/HZSM-5 catalysts was SiO_2/Al_2O_3 ratio of the zeolite. The effects of SiO_2/Al_2O_3 ratio on the Hg^0 and NO removal efficiency were investigated by using 6% Cu/HZSM-5 with the different SiO_2/Al_2O_3 ratios (25, 50 and 100) at 250 °C and the experimental results were shown in Fig. 6.

With the SiO_2/Al_2O_3 ratio increasing, the activity of the 6% Cu/HZSM for the aimed reaction obviously decreased. For instance, only 80% of NO and 60% of Hg^0 removal efficiencies were obtained over the sample with SiO_2/Al_2O_3 ratio of 100, which is considerably lower than 90% of NO and 90% of Hg^0 removal efficiencies obtained over the sample with SiO_2/Al_2O_3 ratio of 25 under the same reaction condition. This result was in good accordance with that observed by other researchers [22–24]. It could be due to copper species incorporated into the channels of the zeolite and occupied the position of the bridging Al–O–Si during the zeolite impregnation procedure. Furthermore, the impregnation procedure could form more number of Cu^+ species and it was essential for good catalytic activity of Cu/HZSM-5 to maintain the balance between Cu^+ and Cu^{2+} species [25]. The aluminum concentration increased resulting in an increase in the Cu^+ concentration of Cu/HZSM-5. Therefore, the more Al in Cu/HZSM-5 was, the higher η_{Hg^0} and η_{NO} of Cu/HZSM-5 would be.

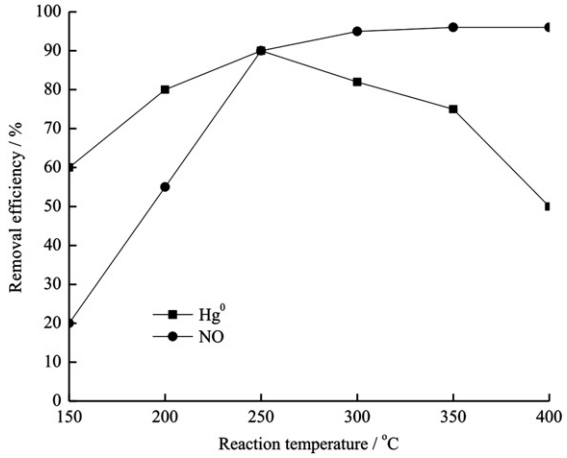

Fig. 4. Effect of reaction temperature on Hg^0 and NO removal efficiencies of 6% Cu/HZSM-5 (25).

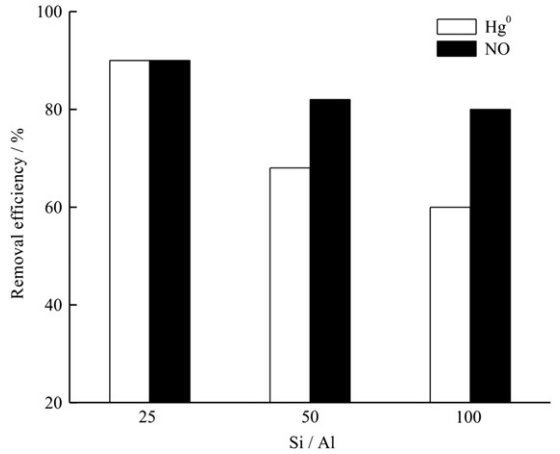

Fig. 6. Effect of the SiO_2/Al_2O_3 ratio on the performance of 6% Cu/HZSM-5 at 250 °C.

3.5. Effect of flue gas components

It has been reported that the presence of flue gas components (like O_2 or H_2O) could influence the removal reaction mechanism of NO and Hg^0 and the nature of the active copper species, which in turn may influence the catalytic activity. To better understand the capture ability of Cu/HZSM-5, the effects of individual flue gas components on the Hg^0 and NO removal efficiencies were examined using 6% Cu/HZSM-5 (25) at 250 °C and the results were illustrated in Fig. 7.

Fig. 7(a) showed the performances of 6% Cu/HZSM-5 (25) on Hg^0 and NO removal efficiencies without adding H_2O and with adding 8% H_2O into the experimental flue gas. The Hg^0 and NO removal efficiencies were inhibited by the presence of water. When H_2O concentration increased from 0 to 8%, the Hg^0 removal efficiency reduced from 90.2% to 82.6% and the NO removal efficiency reduced from 90% to 75.8%. These observations could be explained as due to the competitive adsorption of water [26]. Meanwhile, H_2O was not necessarily mono-layer adsorption. It could fill pores and blocked the sites needed for the aimed reactions to take place, leading to the reduction of the aimed reactions. Fig. 7(b) showed the changes in Hg^0 and NO conversions with respect to O_2 concentration over the 6% Cu/HZSM-5 (25) at 250 °C. It could be seen that an increased oxygen concentration enhanced the NO and Hg^0 removal efficiency. In the absence of O_2, only about 20% Hg^0 removal and 58.4% NO removal efficiencies were achieved; but in the presence of 8% O_2, the Hg^0 and NO removal efficiencies were raised to 90.2% and 90%, respectively. The presence of oxygen has been reported to influence both the reaction mechanism and the nature of the active copper species, which in turn may influence the catalytic activity. Therefore, O_2 in flue gas had a positive effect on the Hg^0 and NO removal. The effects of SO_2 concentration on Hg^0 and NO removal of Cu/HZSM-5 were shown in Fig. 7(c). It could be seen that SO_2 had negative influence on the NO and Hg^0 removals. When the concentration of SO_2 changed from 0 to 900 ppm, the Hg^0 removal efficiency of Cu/HZSM-5 decreased from 90.2% to 72%. Similarly, the NO removal efficiency of Cu/HZS-5 decreased to 75% from the initial level of 90.2% when SO_2 concentration was reached to 900 ppm. That was because SO_2 could compete with NO and NH_3 for the activated sites of the sample surface [27]. On the other hand, copper species was favorable for the storage SO_2 and more active for SO_2 oxidation [28]. This could lead to the formation of ammonium sulfate satls in the presence of NH_3, which might block the activated centers catalyzing Hg^0 and NO conversion and destroy the sample's porous structure due to its sediment.

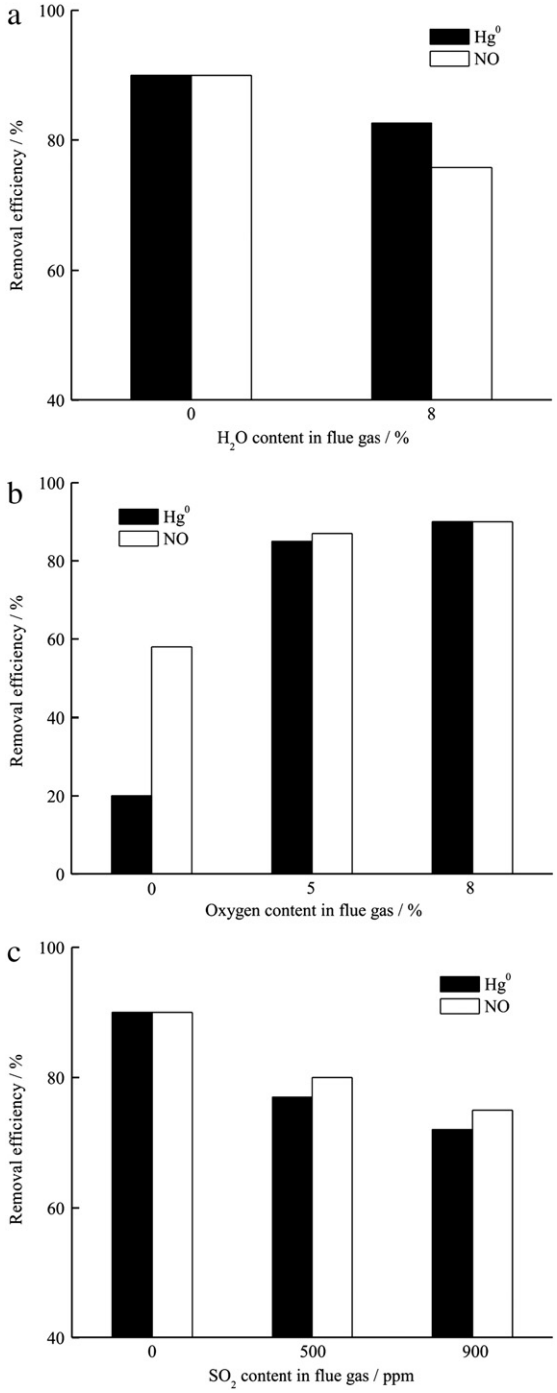

Fig. 7. Effect of flue gas components on the Hg^0 removal efficiency of 6% Cu/HZSM-5 (25) at 250 °C: (a) H_2O, (b) O_2, (c) SO_2.

3.6. Reaction mechanism of the Hg^0 and NO removal

From above experiment, it has been proven that Cu/HZSM-5 not only had higher NO removal efficiency, but also could promote the Hg^0 removal from the flue gas. For the mechanism of NO reduction with NH_3, the overall reaction is usually assumed to involve stoichiometric amounts of NO and NH_3 in the presence of oxygen to produce nitrogen and water [29]. According to this mechanism, first and rate-determining step for the SCR reaction is the oxidation of NO to NO_2 by O_2, because it is more easily reduced by NH_3 than NO [30]. Cu/HZSM-5 which was extensively studied in SCR of NO processes was reported to be a good catalyst for NO oxidation. This was due to the presence of two distinct phases: zeolite and metallic oxide. These phases had different compositions and different physical–chemical properties and in particular different microstructures [31]. Specifically, the NO reduction processes on Cu/HZSM-5 could be expressed as follows: Firstly, gaseous O_2 and NO molecules were adsorbed on the surface of the samples. Then, NO_2 was produced by the interaction between the adsorbed oxygen and NO on CuO sites. On the side, gaseous NH_3 molecules were adsorbed onto the surface of samples. Subsequently, NO_2 molecule react with NH_3 to produce N_2 and H_2O, completing the catalytic cycle.

$$O_2(ad) + NO(ad) \xrightarrow{CuO} NO_2(ad) + O(ad) \quad (3)$$

$$O(ad) + NO(ad) \xrightarrow{CuO} NO_2(ad) \quad (4)$$

$$8NH_3(ad) + 6NO_2(ad) \rightarrow 7N_2 + 12H_2O \quad (5)$$

In order to confirm the mechanism of Hg^0 removal over Cu/HZSM-5, TG analyses of recycling 6% Cu/HZSM-5, which were used at 250 °C in the presence and absence of Hg^0 in the flue gas ($O_2 + N_2$), were shown in Fig. 8. Comparing the weight loss of the samples in the

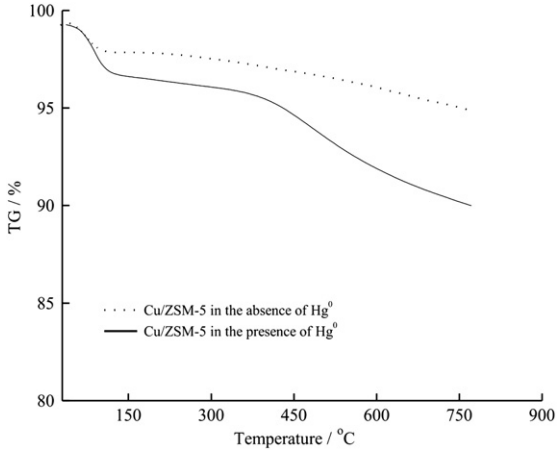

Fig. 8. TG analyses of the samples.

presence and absence of Hg^0, the excess weight loss between 50 °C and 300 °C was attributed to physically adsorption of mercury which was often present as Hg^0 [32]. The other excess weight loss between 400 °C and 600 °C was attributed to chemically oxidation of mercury which was often present as HgO because the thermo decomposition of HgO often took place in the 430 °C–560 °C temperature interval [33]. The results verified that the reaction mechanism of Hg^0 removal was ascribed to the combined action of physically adsorption and chemically oxidation, while chemically oxidation was a dominant process for the Hg^0 capture at 250 °C.

Fig. 4 shows that the Hg^0 removal efficiency of Cu/HZSM-5 enhanced with the increase of reaction temperature. This ascribed to the potentiation of oxidation, which could boost and become the crucial factor with the increase of reaction temperature due to the formation of more chemical bonds between them [34]. However, when the temperature exceeded 250 °C, the Hg^0 removal efficiency would decrease. This could be due to the inhibition of physically adsorption of Hg^0, which could weaken by higher temperature [35]. To be specific, the Hg^0 in the flue gas collided with the sample and was adsorbed on the surface of sample, which ascribed to the physisorption [36]. This physisorption for Hg^0 was mainly dependent upon the acid sites of the surface of the sample, especially Lewis acid sites. Usually, the acidic sites of HZSM-5 were determined by the SiO_2/Al_2O_3 ratio because the Al in the framework of zeolite could form strong acid sites. Moreover, the HZSM-5 modified by copper could lead to a decrease of Bronsted acid sites and an increase of Lewis sites as copper concentration increases [14]. Therefore, the Cu/HZSM-5 with the lower SiO_2/Al_2O_3 ratio could have strongly adsorption for Hg^0 and not be affected by other flue gas component. Secondly, the adsorbed Hg^0 could be oxidized by the active constituent on the sample surface, leading to the formation of new mercury species, which put down to the chemical oxidation [36,37]. Moreover, NO_2 which has been considered as the key intermediate of SCR of NO, also had a promoted effect on the oxidation of Hg^0 [38]. Therefore, Cu/HZSM-5 possessed good reactivity for Hg^0 removal. The detailed procedure of Hg^0 removal over Cu/HZSM-5 could be expressed as follows:

$$Hg^0(ad) + HZSM - 5 \rightarrow Hg^0(ad) \quad (6)$$

$$2Hg^0(ad) + O_2(ad) \xrightarrow{CuO} 2HgO(ad) \quad (7)$$

$$Hg^0(ad) + NO_2(ad) \rightarrow NO(ad) + HgO(ad) \quad (8)$$

Another important challenge, which should be taken into account, is a transport phenomenon since diffusion often limits the activity of the catalysts especially at high reaction rates, which are usually observed in NO SCR with NH_3 [15]. A possible strategy to solve this problem was the introduction of mesopores into the zeolite structure. The presence of an intracrystalline mesopore system in these zeolites has in many cases been shown to help solve diffusion problems. It had been reported that Cu/HZSM-5 catalysts prepared by a simple impregnation procedure and proved the beneficial effect of mesopores on the catalyst activity [39]. Therefore, in some cases, such mesoporous materials could provide better dispersion of the metal component in comparison with microporous systems. Overall, the modification of HZSM-5 by copper for the aimed reaction greatly performed not only the intrinsic property of HZSM-5 and the metals but also the interaction of them.

4. Conclusions

In the present paper, the Hg^0 and NO removal efficiencies of Cu/HZSM-5 were studied in a lab-scale fixed-bed system. Results showed that Cu/HZSM-5 possessed a strong ability for removals of Hg^0 and NO. However, the Hg^0 and NO removal was not beneficial from CuO higher loading value due to the decrease of surface area of Cu/HZSM-5. Moreover, With the SiO_2/Al_2O_3 ratio increasing, the activity of the Cu/HZSM for the aimed reaction obviously decreased. From temperature tests, the Hg^0 removal efficiency of Cu/HZSM-5 enhanced and then decreased with the increase of reaction temperature. But the higher reaction temperature could improve the efficiency of NO conversion. It also concluded that this catalyst could be used in some SCR systems which were downstream of the particulate control device (hot-side ESP), where the catalysts could avoid high-concentration ashes in the flue gas. The flue gas components test showed that O_2 promoted Hg^0 oxidation, while H_2O and SO_2 inhibited Hg^0 removal. Furthermore, the value of NO conversion was strongly promoted by O_2, but inhibited by H_2O and SO_2.

Acknowledgements

This project was supported by the National Natural Science Foundation of China (50878080); the Scientific and Technological Major Special Project of Hunan Province in China (2010XK6003); the National High Technology Research and Development Program of China (863 Program) (No. 2011AA060803) and the Scientific and Technological Major Special Project of Changsha City in China (K0902006-31).

Appendix A. Supplementary data

Supplementary data to this article can be found online at http://dx.doi.org/10.1016/j.fuproc.2012.06.003.

References

[1] S.E. Lindberg, W.J. Stratton, Atmospheric mercury speciation: concentrations and behavior of reactive gaseous mercury in ambient air, Environmental Science and Technology 32 (1998) 49–57.
[2] A.P. Dastoora, Y. Larocpue, Global circulation of atmospheric mercury: a modeling study, Atmospheric Environment 38 (2004) 147–161.
[3] T.D. Brown, D.N. Smith, R.A. Hargis, Mercury measurement and its control: what we know, have learned, and need to further investigate, Journal of the Air & Waste Management Association 49 (1999) 628–640.
[4] Y. Wu, S.X. Wang, D.G. Streets, Trends in anthropogenic mercury emissions in China from 1995 to 2003, Environmental Science and Technology 40 (2006) 5312–5318.
[5] G. Skodras, Ir. Diamantopoulou, G. Pantoleontoc, G.P. Sakellaropoulos, Kinetic studies of elemental mercury adsorption in activated carbon fixed bed reactor, Journal of Hazardous Materials 158 (2008) 1–13.
[6] J. Bustard, M. Durham, T. Starns, C. Lindsey, C. Martin, R. Schlager, Full-scale evaluation of sorbent injection for mercury control on coal-fired power plants, Fuel Processing Technology 85 (2004) 549–562.
[7] J.H. Pavlish, M.J. Holmes, S.A. Benson, C.R. Crocker, K.C. Galbreath, Application of sorbents for mercury control for utilities burning lignite coal, Fuel Processing Technology 85 (2004) 563–576.
[8] S.J. Wu, M.A. Uddin, E. Sasaoka, Characteristics of removal of mercury vapor in coal derived fuel gas over iron oxide sorbents, Fuel 85 (2006) 213–218.

[9] G. Dunham, R. Dewall, C. Senior, Fixed-bed studies of the interactions between mercury and coal combustion fly ash, Fuel Processing Technology 82 (2003) 197–213.
[10] H. Kamata, S.I. Ueno, N. Sato, T. Naito, Mercury oxidation by hydrochloric acid over TiO_2 supported metal oxide catalysts in coal combustion flue gas, Fuel Processing Technology 90 (2009) 947–951.
[11] X.P. Fan, C.T. Li, G.M. Zeng, X. Zhang, S.S. Tao, P. Lu, Y. Tan, D.Q. Luo, Hg^0 removal from simulated flue gas over CeO_2/HZSM-5, Energy & Fuels 26 (2011) 2082–2089.
[12] N.Q. Yan, W.M. Chen, J. Chen, Z. Qu, Y.F. Guo, S.J. Yang, J.P. Jia, Significance of RuO_2 modified SCR catalyst for elemental mercury oxidation in coal-fired flue gas, Environmental Science and Technology 45 (2011) 5725–5730.
[13] Z.J. Mei, Z.M. Shen, Z.Y. Mei, Y.J. Zhang, F. Xiang, J.P. Chen, W.H. Wang, The effect of N-doping and halide-doping on the activity of $CuCoO_4$ for the oxidation of elemental mercury, Applied Catalysis B: Environmental 78 (2008) 112–119.
[14] Y. Zhuang, J. Laumb, R. Liggett, M. Holmes, J. Pavlish, Impacts of acid gases on mercury oxidation across SCR catalyst, Fuel Processing Technology 88 (2007) 929–934.
[15] L. Ji, P.M. Sreekanth, P.G. Smirniotis, S.W. Thiel, N.G. Pinto, Manganese oxide/titania materials for removal of NO_x and elemental mercury from flue gas, Energy & Fuels 22 (2008) 2299–2306.
[16] M.H.O. Nunes, V.T.D. Silva, M. Schmal, The effect of copper loading on the acidity of Cu/HZSM-5 catalysts: IR of ammonia and methanol for methylamines synthesis, Applied Catalysis A: General 294 (2005) 148–155.
[17] M.Y. Kustova, S.B. Rasmussen, A.L. Kustov, C.H. Christensen, Direct NO decomposition over conventional and mesoporous Cu-ZSM-5 and Cu-ZSM-11 catalysts: improved performance with hierarchical zeolites, Applied Catalysis B: Environmental 67 (2006) 60–67.
[18] H. Sjovall, L. Olsson, E. Fridell, R.J. Blint, Selective catalytic reduction of NO_x with NH3 over Cu-ZSM-5—the effect of changing the gas composition, Applied Catalysis B: Environmental 64 (2006) 180–188.
[19] L. Chen, C.T. Li, Z. Gao, X.P. Fan, Experimental study of removing elemental mercury from flue gas by MnOx/HZSM-5, Journal of Environmental Sciences (China) 30 (2010) 1026–1031 (in Chinese).
[20] Y. Akimasa, A. Hiroyuki, I. Shigeo, Mercury oxidation by copper oxides in combustion flue gases, Powder Technology 180 (2007) 222–226.
[21] X.P. Fan, C.T. Li, G.M. Zeng, L.H. Tian, Z. Gao, Experimental research of removing elemental mercury from flue gas by CuO–CeO_2/AC, Journal of Environmental Engineering 4 (2010) 103–107 (In chinese).
[22] S.Y. Chen, Y.C. Zhang, X.W. Guo, Adsorption removal of trace NO from a CO_2 stream over transition-metal-oxide-modified HZSM-5, Separation and Purification Technology 69 (2009) 288–293.
[23] R. Bi, X.P. Wang, Z.G. Liu, J. Chen, Effect of dispersion and distribution of tungsten on W/HZSM-5 for selective catalytic reduction of NO by acetylene, Journal of Natural Gas Chemistry 17 (2008) 332–336.
[24] J. Liu, C.X. Zhang, Z.H. Shen, W.M. Hua, Y. Tang, W. Shen, Y.H. Yue, H.L. Xu, Methanol to propylene: effect of phosphorus on a high silica HZSM-5 catalyst, Catalysis Communications 10 (2009) 1506–1509.
[25] A. Sultana, T. Nanba, M. Haneda, M. Haneda, M. Sasaki, H. Hamada, Influence of co-cations on the formation of Cu^+ species in Cu/ZSM-5 and its effect on selective catalytic reduction of NO_x with NH_3, Applied Catalysis B: Environmental 101 (2010) 61–67.
[26] P. Park, C.L. Boyer, Effect of SO_2 on the activity of Ag/γ-Al_2O_3 catalysts for NO_x reduction in lean conditions, Applied Catalysis B: Environmental 59 (2005) 27–34.
[27] M. Casapu, O. Krocher, M. Elsener, Screening of doped MnO_x–CeO_2 catalysts for low-temperature NO-SCR, Applied Catalysis B: Environmental 88 (2009) 413–419.
[28] X.P. Wang, S.X. Zhang, Q. Yu, H.L. Yang, Tungsten promoted HZSM-5 in the SCR of NO by acetylene, Microporous and Mesoporous Materials 109 (2008) 298–304.
[29] L.L. Ren, T. Zhang, J.W. Tang, J.F. Zhao, N. Li, L.W. Lin, Promotional effect of colloidal alumina on the activity of the In/HZSM-5 catalyst for the selective reduction of NO with methane, Applied Catalysis B: Environmental 41 (2003) 129–136.
[30] N. Mongkolsiri, P. Praserthdam, P.L. Silveston, R.R. Hudgins, Transient study of the effect of residual cations in Cu/ZSM-5 for SCR of NO by hydrocarbon, Chemical Engineering Science 55 (2000) 2249–2256.
[31] A. Sultana, T. Nanba, M. Haneda, H. Hamada, SCR of NO_x with NH_3 over Cu/NaZSM-5 and Cu/HZSM-5 in the presence of decane, Catalysis Communications 10 (2009) 1859–1863.
[32] S. Poulston, E.J. Granite, H.W. Pennline, C. Myers, Metal sorbents for high temperature mercury capture from fuel gas, Fuel 86 (2007) 2201–2203.
[33] M. Lopez-Anton, Y. Yuan, R. Perry, M. Maroto-Valer, Analysis of mercury species present during coal combustion by thermal desorption, Fuel 89 (2010) 629–634.
[34] H.C. Zeng, F. Jin, J. Guo, Removal of elemental mercury from coal combustion flue gas by chloride-impregnated activated carbon, Fuel 83 (2004) 143–146.
[35] Y.H. Li, C.W. Lee, B.K. Gullett, Importance of activated carbon's oxygen surface functional groups on elemental mercury adsorption, Fuel 82 (2003) 451–457.
[36] X.P. Fan, C.T. Li, G.M. Zeng, Z. Gao, L. Chen, Removal of gas-phase element mercury by activated carbon fiber impregnated with CeO_2, Energy & Fuels 24 (2010) 4250–4254.
[37] J.W. Graydon, X.Z. Zhang, D.W. Kirk, C.Q. Jia, Sorption and stability of mercury on activated carbon for emission control, Journal of Hazardous Materials 168 (2009) 978–982.
[38] H.L. Li, C.Y. Wu, Y. Li, J.Y. Zhang, CeO_2–TiO_2 catalysts for catalytic oxidation of elemental mercury in low-rank coal combustion flue gas, Environmental Science and Technology 45 (2011) 7394–7400.
[39] A.L. Kustov, T.W. Hansen, M. Kustova, C.H. Christensen, Selective catalytic reduction of NO by ammonia using mesoporous Fe-containing HZSM-5 and HZSM-12 zeolite catalysts: an option for automotive applications, Applied Catalysis B: Environmental 76 (2007) 311–319.